Impact of varying macronutrient composition on the printability of pea-based inks in extrusion-based 3D food printing

Aaditya Venkatachalam [a], Ajay Balasubramaniam [b], Patrick F.C. Wilms [a], Lu Zhang [a], Maarten A.I. Schutyser [a,*]

[a] Laboratory of Food Process Engineering, Wageningen University, Bornse Weilanden 9, 6708WG, Wageningen, PO Box 17, the Netherlands
[b] Advanced Research Laboratory, NavInfo Europe B.V, 5657DB, Eindhoven, the Netherlands

ARTICLE INFO

ABSTRACT

Personalized foods with varying macronutrient compositions can be created by 3D food printing to fulfill the dietary requirements of individual consumers. In this work, we aim to quantitatively study the influence of varying multiple macronutrient concentrations on printability of food inks, by applying a systematic approach. Pea-based food inks consisting of insoluble pea fibre, pea protein, and native pea starch were formulated and water was added following these ingredients' respective water holding capacities. Printability was quantified in terms of extrudability (force required to extrude material out of a cartridge), buildability (flow point to determine shape stability after deposition on the printing platform), and printing precision (surface defect index (SDI) of the printed object). This approach helps to efficiently define a printable landscape of pea-based inks with a large variation in macronutrient composition. Our results show that increasing protein concentration resulted in increased extrusion force and flow point, while the opposite effect was found for fibre. Of all the tested pea-based formulations, 71% could be printed to a height of 50 mm with high printing precision (SDI<0.14). The presented systematic approach provides a solid basis for rapid development of printable plant-based inks while avoiding a trial-and-error approach to optimize inks with highly variable macronutrient composition.

1. Introduction

Personalized nutrition has been proven to help people adapt to a healthier diet compared to the conventional 'one size fits all' non-personalized method (Celis-Morales et al., 2016). Extrusion-based 3D Food Printing (3DFP) is an emerging technology that has the potential to develop tailor-made personalized foods (Pereira, Barroso, & Gil, 2021) for people who require specialized nutrition such as elderly, athletes, and dysphagia patients. Dysphagia patients, who suffer from swallowing problems, require texture-modified foods to ensure safe consumption (Lorenz, Iskandar, Baeghbali, Ngadi, & Kubow, 2022; Sura, Madhavan, Carnaby-Mann, & Crary, 2012). In recent years, texture-modified foods have often been realized through 3DFP. Apart from these distinct consumer groups, personalized nutrition also benefits healthy people who desire to add or eliminate specific micro- and macronutrients in their regular diet. This can be due to particular dietary preferences or to consume specific nutrients based on body requirements (Ordovas, Ferguson, Tai, & Mathers, 2018). For instance, a healthy person with

reduced levels of blood hemoglobin may choose to consciously increase iron levels in their diet. By changing the amount of micro- and macronutrients used in a formulation, the nutritional content of foods can be varied.

Macronutrients such as carbohydrates, proteins, and fats make up a major part of the formulation. The food ingredients and their respective macronutrient compositions influence the printability of a material. In extrusion-based 3DFP, a food ink is pushed through a nozzle onto a printing platform using a piston/air pressure. Ideally, the ink has to overcome a certain yield stress and possesses shear-thinning properties to facilitate flow through the cartridge into the nozzle. This is referred to as the extrudability of the sample (Wilms et al., 2021). During dispensing a self-supporting structure is built up layer by layer. The ability of a material that allows building of such a structure is referred to as buildability (Wilms et al., 2021). Extrudability and buildability together determine the printability. Researchers have explored quantitative predictive models for different formulations with varying rheological properties to predict the extrudability of inks

([Ma, Schutyser, Boom, & Zhang, 2021](#)) and correlations between the rheological properties of formulations and shape stability ([Zhu, Stieger, van der Goot, & Schutyser, 2019](#)). They found that materials which exhibited stronger shear-thinning behavior required lower printing pressures to print an object. Printing pressure in turn was successfully used to predict extrudability ([Ma et al., 2021](#)) and flow point was found to have a linear correlation with printing stability ([Zhu et al., 2019](#)). These studies used either pre-made ready-to-eat foods or a system consisting of a single macronutrient to arrive at these conclusions. However, to design a nutritious personalized meal, it is important to use a formulation with multiple macronutrients and gather quantitative insights on the printability of these formulations.

Designing formulations with multiple macronutrients is complicated and conventionally involves a series of trial-and-error steps to achieve a printable ink. Formulations are typically made by varying the percentage of macronutrients including added water. Water behaves as a plasticizer and is responsible for achieving a printable ink ([Zhang, Lou, & Schutyser, 2018](#)). By varying the amount of water, printability of these water-based food inks can be altered ([Godoi, Prakash, & Bhandari, 2016](#); Y. [Liu, Zhang, & Ye, 2020](#); [Zhang et al., 2018](#)). Such an adjustment is usually performed on wet basis. For instance, [He, Zhang, and Guo (2020)](#) made purple mashed potato puree by mixing 22.73% purple sweet potato powder and 1.52% sodium alginate powder with boiling water. If printing this ink results in over-extrusion or oozing, it is common practice that the recipe is corrected by varying the amount of water until a good print is obtained. When working with a single macronutrient system such an optimization might be straightforward. However, this optimization would get rather complex in a multiple macronutrient system and also when ingredient sources are varied. For these variations in macronutrients, it is hard to predict the water absorption and binding. Therefore, a novel guideline for formulation design is needed to get quickly to a printable ink.

The aim of this study was to quantitatively investigate the effect of varying macronutrients carbohydrates (fibre and starch) and proteins on printability of water-based formulations, using an experimental design approach. Given the relevance of plant-based materials for sustainable food production and the high nutritional value of pea ([Barac et al., 2010](#)), a pea-based model ink consisting of insoluble pea fibre, native pea starch, and pea protein was investigated. An additional advantage of pea is that its components are readily available as ingredients. Native starch was preferred over gelatinized starch to allow for larger variations in starch content as the use of gelatinized starch may quickly lead to clogging at higher concentrations. Firstly, water holding capacity (WHC) of the pea-based ingredients was measured. Secondly, multiple formulations were made by varying macronutrient composition using a rationale of adding water based on the WHC of the individual ingredients. Thereafter, the formulated inks were tested for printability by means of extrudability, buildability, and printing precision. This was carried out by measuring force to extrude, flow point, and surface defect index, respectively. By doing so, printable formulations were achieved with minimum trial-and-error and a printability landscape was constructed. Using this knowledge, in the future, printable plant-based food inks for creating personalized foods can be better designed.

2. Materials and methods

2.1. Materials and physical properties characterization

A pea-based model ink system containing three ingredients namely: insoluble fibre, native starch, and protein were used in this study. Swelite™ C Pea Fiber (48% fibre on dry basis (db)), Nastar™ Native Pea Starch (99% starch db), and Pisane™ M9 Pea Protein (85.3% protein db) were kindly provided by Cosucra Groupe Warcoing SA, Belgium. The composition of each ingredient mentioned within brackets is reported based on manufacturer specifications. Physical properties of these three ingredients were characterized in terms of moisture content and WHC.

2.1.1. Moisture content

Dry ingredients of mass 2.000g were weighed into the petri-dish and subsequently, the samples were placed in a hot air oven at 105 °C for 24h. The difference in weight was used to calculate moisture content on db. All measurements were triplicated.

2.1.2. Water holding capacity (WHC)

WHC was measured using the method reported by [Geerts, Dekkers, van der Padt, and van der Goot (2018)](#). 2% (w/v) of all dry ingredients [$M_{dry\ ingredient}$] were dispersed in demineralized water and agitated for 24 h at 800 rpm using a shaker (Heidolph Multi Reax, Germany) at ambient temperature. Dispersions were then centrifuged using Syrvall Lynx 4000 (Thermo Scientific, Waltham, United States) at a speed of 10,000 rpm at 25 °C for 30 min. Subsequently, the supernatant was separated, and the wet samples were transferred to a petri-dish, weighed [$M_{wet\ sample}$], and dried overnight using a hot air oven at 105 °C for 24 h [$M_{dried\ sample}$]. WHC (kg/kg) was determined using Eq [(1)](#). All measurements were triplicated.

$$WHC = \frac{M_{wet\ sample} - M_{dried\ sample}}{M_{dry\ ingredient}} \qquad (1)$$

2.2. Experimental design

Using the measured moisture content and WHC values of the dry ingredients, water required to make printable inks was calculated. Doing so, it was ensured that the formulation did not have an excess amount of unbound water. Based on preliminary printing results (see [Appendix A.1](#). Supplementary data), 27% of each ingredients' WHC was found to be suitable to formulate printable inks. Therefore, to understand the effect of varying the three dry ingredients on printability, multiple formulations were made ([Fig. 1](#)) by adding 27% of each ingredients' WHC as water. Eq [(2)](#) was used to determine the amount of added water (kg) to make a formulation:

$$W_{add} = 0.27 \bullet [WHC_F \bullet M_F + WHC_S \bullet M_S + WHC_P \bullet M_P] - [X_F \bullet M_F + X_S \bullet M_S + X_P \bullet M_P] \qquad (2)$$
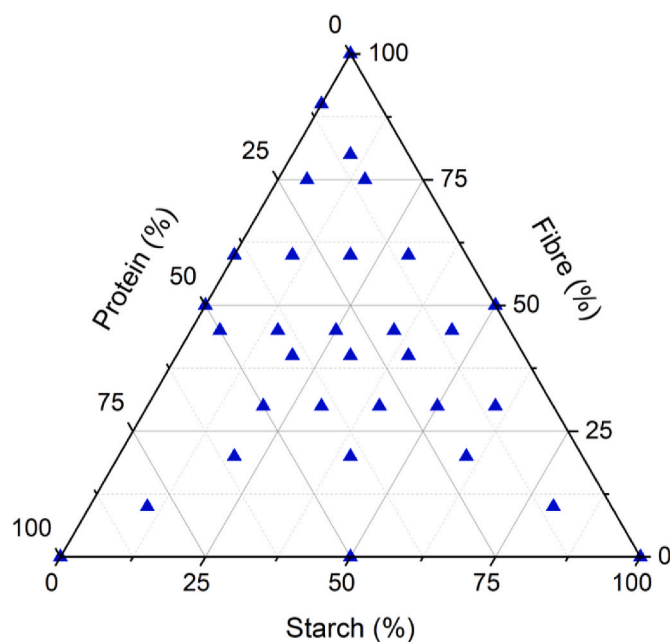

Fig. 1. Experimental design created by varying the amount of fibre, starch, and protein on dry basis to understand the effect of varying macronutrient composition on printability.

Here, M is the dry mass of an ingredient i.e. the mass of the dry ingredient after subtracting the mass of the water fraction in the powder (kg db), X is the moisture content of the powder ingredient on dry basis (kg/kg db), and F, S, and P represent subscripts of fibre, starch, and protein in the formulation, respectively.

Samples were named based on the amount of fibre, starch, and protein content on dry basis. For example, a sample containing 60%w/w db fibre, 20%w/w db starch, and 20%w/w db protein was named as F60S20P20.

2.3. Pea-based inks preparation and characterization

2.3.1. Sample preparation

Based on the formulation, the calculated amount of water was weighed and added into a kitchen mixer (Kenwood Kitchen Mixer, UK). Dry ingredients were weighed, manually pre-mixed using a spoon and subsequently added into the mixer containing water. The formulation was mixed for 5 min with a lid covering the opening of the mixer to prevent moisture loss. Then, air was removed from the samples using a planetary vacuum mixer (Thinky Vacuum Mixer ARV-310LED, USA) at a speed of 2000 rpm with a pressure of 30 kPa for 2 min at ambient temperature. After vacuuming the samples, a parafilm was used to cover the hole on the vacuum cups to avoid further moisture loss during storage. Finally, the samples were stored overnight in a refrigerator at 4 °C. Samples were kept at room temperature 1 h prior to performing further measurements.

2.3.2. Confocal laser scanning microscopy (CLSM)

Samples F80S10P10, F20S40P40, F50S0P50, and F20S60P20 were prepared as described in the previous section. A small amount of the sample was spread evenly on to a glass slide. Subsequently, the sample was stained with 0.5 ml dye made using a combination of 0.005% Calcofluor White (FB28), 0.05% Fluorescein isothiocyanate (FITC), and 0.04% FastGreen (FCF) dyes which have an affinity for fibre, starch, and protein used in the formulations, respectively. Once stained, the glass slide was stored in the refrigerator overnight and used the next day to study the microstructure of the sample. The sample was visualized under an inverted DMi8 CS Confocal Laser Scanning Microscope (Stellaris 8, Lecia Microsystems CMS GmbH, Germany). An objective magnification of HC PL APO CS2 20x/0.75 DRY with excitation wavelengths of 405 nm, 495 nm, and 631 nm were used to record the pictures.

2.4. Printability analysis

The experimental workflow of this study is shown in Fig. 2. The formulated inks were initially visually assessed. Only when a pasty structure was observed, the samples were further analyzed in terms of extrudability—see 2.4.1. Furthermore, samples having an extrusion force value higher than 800N were not printable as the maximum force of the printer would be exceeded. Hence, samples requiring a lower extrusion force than 800N were tested to check if these could be printed to a height of 50 mm. Printing experiments were performed using a Procusini 5.0 Food Printer (Procusini, Germany). Samples were loaded into a metal cartridge (Ø = 27 mm) to minimize entrainment of air. All samples were printed using a tapered nozzle (Ø = 1.2 mm) at room temperature. Printing settings such as printing speed (38% i.e., 15 mm/s (calculated value)), layer height (0.55 mm), infill density (25%), and retraction (0 mm) were kept constant. The samples were printed in the shape of a hollow cuboid having 40 × 40 × 50 mm dimensions. If a sample could not be printed up to 50 mm height, samples were categorized having a qualitative defect and not further evaluated. If a sample could be printed to a height of 50 mm, buildability and printing precision were measured—see 2.4.2 and 2.4.3, respectively.

2.4.1. Extrudability

A similar set-up as reported by Zhu et al. (2019) was used to measure the force needed to extrude the food ink. A universal testing machine (Instron Texture Analyser, USA) having a 2000 N load cell (Ø = 0.5 mm) was used. Samples were filled into the same metal cartridge used for the printability analysis, to which the same tapered nozzle (Ø = 1.2 mm) was attached. Subsequently the samples were allowed to rest for 2 min, after which the probe was manually displaced until continuous flow was visible. Following this, the probe was moved 5 mm upwards at a constant speed of 0.05 mm/s and allowed to relax for 90s so that the material recovers back to its original state. Thereafter, the probe was displaced 15 mm downward at a constant speed of 0.03 mm/s to measure the force required to extrude the sample. This speed corresponds to a printing speed of 15 mm/s which was calculated using the continuity equation as proposed by Moretti, Rossi, and Senin (2021). From these measurements, the average equilibrium force value was calculated and reported similar to the methodology reported by Zhu et al. (2019). Measurements were performed in duplicate. The relative standard deviation of all the measured formulations did not exceed 26.2% with the average value being 6.28%.

2.4.2. Buildability

To determine the force at which the material starts to lose its shape stability, the flow point was measured by performing an amplitude sweep test using a rheometer (Anton Paar MCR 301 Rheometer, Anton Paar GmbH, Austria). Since the formulations used had a pasty structure, a corrugated plate-plate geometry (Ø = 25 mm) was used. A gap of 1.5 mm was set to measure the sample. Once the sample was loaded on the
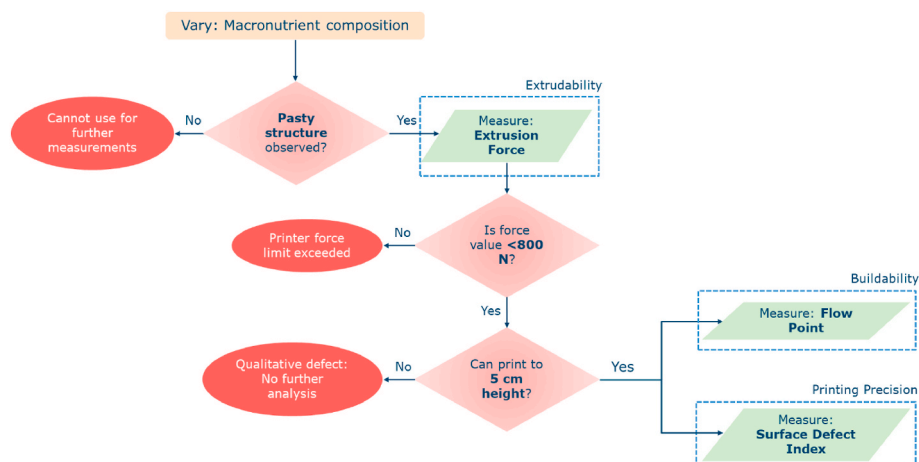

Fig. 2. Workflow used in this study to quantify printability of pea-based inks.

plate, paraffin oil was used to coat the edges to avoid dehydration of the sample during the measurement. Furthermore, the sample was allowed to rest for 2 min at 20 °C before proceeding to perform a strain sweep test. Shear strain was varied from 0.01 to 100% at a fixed frequency of 1Hz and temperature of 20 °C. The point at which G′ and G″ crossed over was determined as the flow point which was correlated to the shape stability of the printed sample (Liu, Bhandari, Prakash, Mantihal, & Zhang, 2019; Zhu et al., 2019). Measurements were performed in duplicate. The relative standard deviation did not exceed 11.7% with an average value of 2.6%.

2.4.3. Printing precision

A surface defect index of a printed sample was defined in this study as a measure for the printing precision of food inks. After printing samples to a height of 50 mm, images were taken using a Sony FDR-AX53 4K Handycam® with Emor R™ CMOS sensor (Sony Corporation, Japan). The images were processed using Imaging Web Demonstrations (Biomedical Imaging Group, EPFL) canny edge detector and structural information of pictures of printed samples was obtained. For the canny edge detector, a hysteresis threshold with a sigma value of 2 was applied. Low and high resolution was set to 0% and 3%, respectively. The number of detected edges was quantified in terms of number of white pixels in the image using a python script. The surface defect index (SDI) is calculated by comparing the number of detected white pixels from edges for each printed sample to that of a reference (printed white chocolate–Procusini® 3D Choco White) using Eq (3).

$$SDI = \frac{N_{max} - N}{N_{max}} \tag{3}$$

N represents the number of white pixels counted in the image of the printed sample. N_{max} represents 3D printed white chocolate which is a food material that can be printed with high precision leading to more detected edges and thus high white pixel number compared to the other printed samples.

2.5. Data analysis

Data analysis was performed using Python 3.9 (64-bit) and graphs were made using Origin 2022b, OriginLab Corporation, USA.

3. Results and discussion

3.1. Characterization of dry ingredients and food inks

3.1.1. Physical properties of dry ingredients

Physical properties of dry ingredients were characterized in terms of moisture content and WHC (see Table 1). Insoluble fibre had the highest WHC, followed by protein and native starch. WHC is the property of a material to prevent the release of its own and added water when external forces are applied, for instance during pressing or centrifugation (Zayas, 1997). In a structured food matrix, water is present in different forms: as free water, bound water, and trapped water. Free water can be easily removed by gravity or mechanical force. Conversely, bound and trapped water are comparatively difficult to remove. Bound water is absorbed to the macromolecules while trapped water is retained between macromolecules causing it to lose motional freedom (Kneifel, Paquin, Abert, & Richard, 1991; Zayas, 1997). WHC varies based on the composition and

conformation of the raw materials used. Previous research showed water content to significantly influence the rheological properties and printability of food inks (Y. Liu, Zhang, & Ye, 2020; Zhang et al., 2018). Therefore, determining WHC of dry ingredients provides useful information for food ink design.

3.1.2. Microstructure of pea-based food inks

CLSM images were made to visualize the microstructure of the different pea-based food inks containing fibre, starch, and protein stained in blue, green, and red, respectively. Four representative formulations were chosen with as much composition variation as possible (F80S10P10, F30S30P40, F50S0P50, F20S60P20) (see Fig. 3). When a formulation was dominated by fibre (80%w/w db) (Fig. 3A), it was observed that components fibre, starch, and protein were dispersed more unevenly within the matrix at the microscopic scale. However, at a macroscopic scale, these inhomogeneities were not visible. Fibre fibrils appear to have some closed cavities in which water may be entrapped. Most fibers contain hydroxyl groups onto which water molecules can be attached through hydrogen bonds (Boulos, Greenfield, & Wills, 2000; Hearle, 1962). Due to the dipolar nature of water, the first layer is assumed tightly bound to specific polar hydrophilic sites of the fibre molecule. This is followed by a loosely bound multi-polarized second layer of water that is adsorbed on to the surface of the fibre (Boulos et al., 2000; Hearle, 1962; Zayas, 1997). It is expected that when force is applied, these cavities break easily, releasing the water that is trapped between them.

A more homogeneous system was observed with a large concentration of pea proteins (40%w/w db) (Fig. 3B). Pea proteins contain polypeptide groups on to which water molecules are attached through hydrogen bonding (Zayas, 1997). These proteins absorb water and disentangle to form the continuous phase of the matrix in which starch and fibre are dispersed unevenly. With increasing protein content, the strength of the continuous matrix increases (Wang et al., 2020). It is therefore expected that there will be a positive relationship between protein content and extrusion force.

The observation concerning the absorption of water was confirmed by the samples with equal amounts of fibre and protein, but without starch (Fig. 3C). The proteins formed the continuous phase while fibre fibrils are distributed within the protein matrix. It would be interesting to quantify the water distribution between fibre and protein using Nuclear Magnetic Resonance (NMR) to better understand the water absorption and redistribution within a mixture, similar to the study of Dekkers et al. (2016). This, however, is beyond the scope of this study. When a large amount of starch (60%w/w db) was added to the formulation (Fig. 3D), a higher number of starch granules was present in the dispersed phase. This is because native starch is not soluble in cold water. Because formulations were made at room temperature, starch granules lacked hydrophilicity. This lack of hydrophilicity probably prevents water from penetrating deep into the starch granules, which further results in lower water absorption compared to both fibre and protein. Therefore, it is hypothesized that samples with high starch would have a higher extrusion force.

Overall, these CLSM images show that the microstructure of pea-based inks varies with varying macronutrient composition. It seems that pea protein was able to absorb water and form the continuous phase while fibre and native starch granules acted as fillers. These microstructural changes are expected to affect the rheological properties of the inks and thus their printing performance.

3.2. Effect of varying macronutrient content on printability

3.2.1. Extrudability

The ability of a material to flow through a nozzle is called extrudability (Wilms et al., 2021), and can be characterized by measuring the extrusion force of a material (Zhu et al., 2019). In our tests, extrusion force values were only measured for samples visually assessed as pasty,
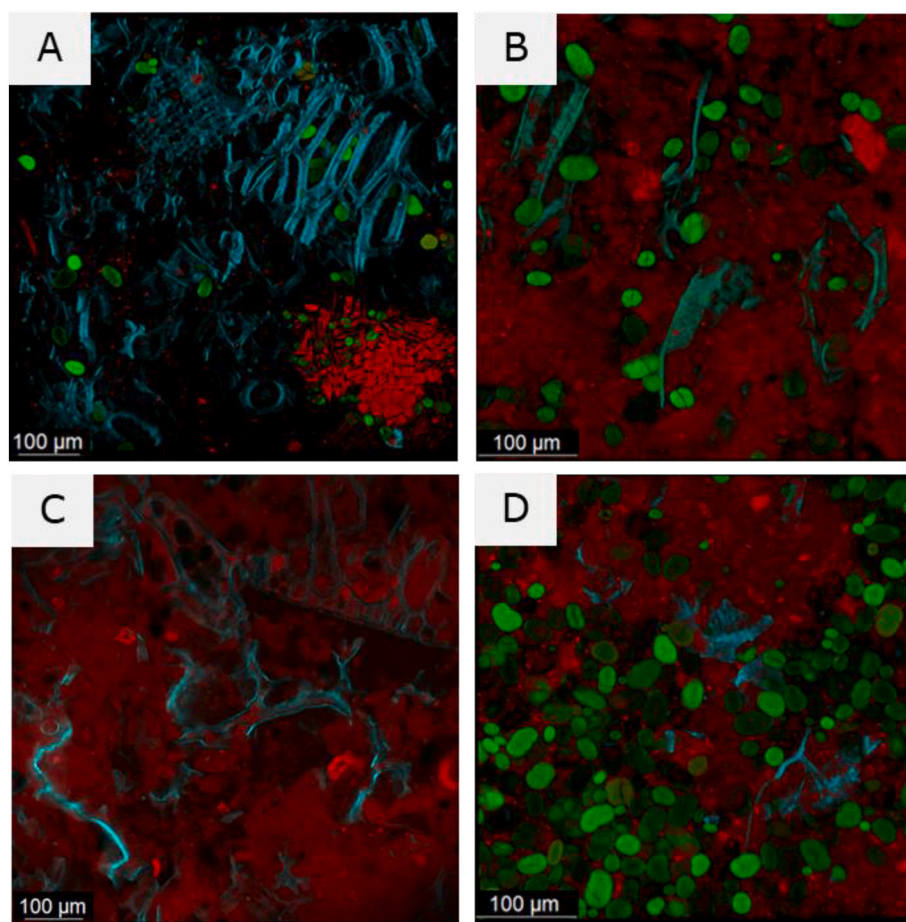
Table 1
Characterization of moisture content and water holding capacity (WHC) of the dry ingredients used in this study.

	Moisture Content (% db)	WHC (kg/kg db)
Fibre (Insoluble)	11.77 ± 0.04	10.99 ± 0.03
Protein	4.08 ± 0.03	5.05 ± 0.03
Starch (Native)	11.71 ± 0.03	1.05 ± 0.05

Fig. 3. CLSM images of samples F80S10P10 (A), F30S30P40 (B), F50S0P50 (C), and F20S60P20 (D). F, S, and P represent insoluble fibre, native starch, and protein which are stained in blue, green, and red, respectively.

i.e. the material was cohesive, stuck to a spoon, and was not crumbly. These pasty samples contained fibre (20–80%w/w db), protein (20–80% w/w db), and starch (0–60%w/w db). These formulations were measurable for force values and are represented by blue triangles in Fig. 4. Force values were not reported for samples that could not be extruded, due to either phase separation or attainment of instrumental force limit (1990N). The phase separated samples had 0%w/w db protein and >80%w/w db fibre content. The samples whose force limit was >1990N contained <20%w/w db fibre, >80%w/w db protein, and >60%w/w db starch are represented by red triangles (unmeasurable formulations) in Fig. 4.

Extrusion force value of the measurable pasty samples reached a plateau (for example see F40S30P30 in Fig. 5), indicating that an equilibrium was attained. The measured equilibrium extrusion force values by varying macronutrient content were plotted in a ternary plot (Fig. 4). In this plot, a change in color gradient from white, yellow, red, to grey corresponds to an increase in extrusion force. With an increase in fibre content, extrusion force decreased. However, when the fibre content was increased beyond 80%w/w db, the profile of extrusion force did not show a plateau (Fig. 5). This means the force value did not reach an equilibrium at this high fibre content, which is most likely due to phase separation of water from the matrix. O'Neill et al. (2017) described a similar observation for calcium phosphate pastes used in clinical applications. One of their proposed hypotheses for phase separation was filtration. During filtration, pressure applied on the liquid phase is relatively higher than the permeability of the particle network, leading to phase separation. The same phenomenon may explain the observations for the fiber-rich systems in this study. The water less tightly bound within the matrix may move faster than the macronutrients and could
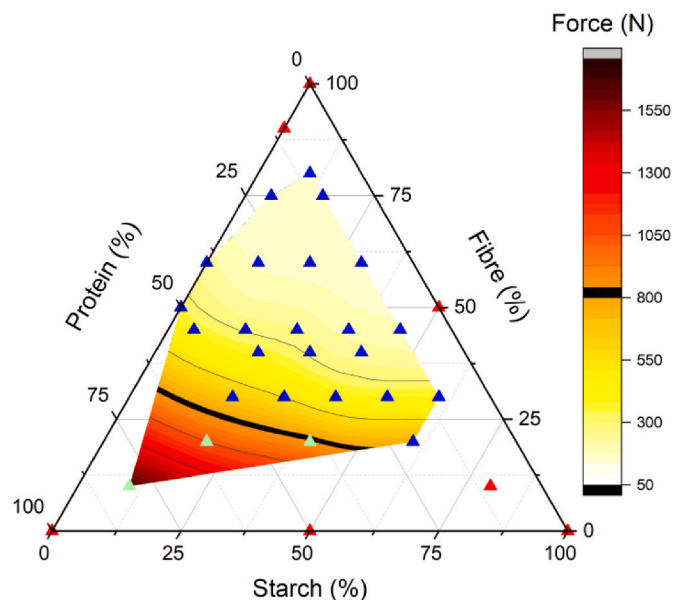

Fig. 4. The effect of varying formulations containing pea-based macronutrients, namely fibre, starch, and protein on the extrusion force of material when extruded through a 1.2 mm nozzle. Compositions are given in weight percentages on dry basis. The ternary plot shows the extrusion force values of measurable formulations ▲, unmeasurable formulations ▲, and formulations with force >800N ▲. The solid line — depicts the 800N extrusion force threshold.
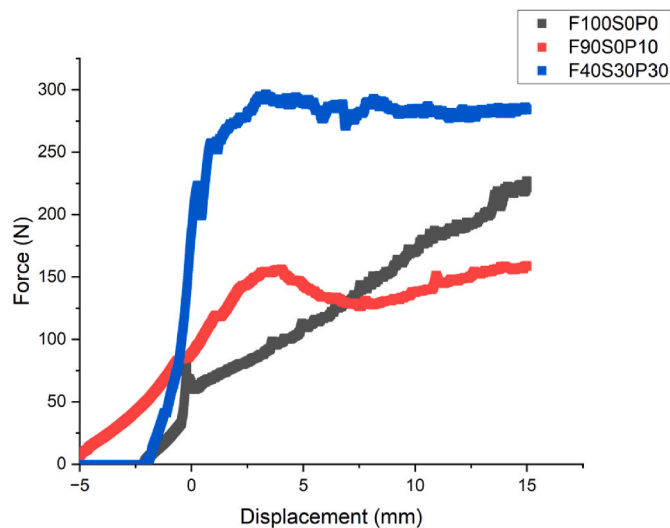
Fig. 5. Representative force-displacement profiles of samples varying in fibre content.

lead to the observed phase separation. This filtration phenomenon could result in a dry-matter gradient within the cartridge and further result in a gradual increase in the force required to extrude (Fig. 5). Subsequently, when more force is applied to extrude the remaining dry matter content, even more water is released, further increasing the dry matter content. Thus, the force value continues to increase over time without reaching an equilibrium value. This phenomenon was also observed when the protein content was low (approx. 0–10%w/w db protein) in the formulation. With an increase in protein content (10–80%w/w db), an increase in extrusion force was observed (Fig. 4). Based on CLSM images, it is hypothesized that proteins absorbed water and disentangled to form a continuous gelled phase. Hence, with an increase in protein content, an increase in viscosity of the continuous phase will lead to the observed increase in extrusion force.

Native starch was observed to have no significant effect on extrusion force at the concentrations used in this study (Fig. 4). However, it has almost always been reported to have an influence on printing characteristics (Chuanxing, Qi, Hui, Quancheng, & Wang, 2018; He et al., 2020; Liu, Zhang, & Ye, 2020). Most of these previous 3D printing studies employed gelatinized starch by heating it to temperatures of 60 °C and above. In this study, native pea starch was used at concentrations between 0 and 60%w/w db without heating. Therefore, native starch granules are likely acting as inert fillers inside the suspension, rather than as a thickening agent.

3.2.2. Buildability

Extrudable formulations made with 20–80%w/w db fibre, 10–50% w/w db protein, and 0–60%w/w db starch had force values less than 800N (samples above the solid line in Fig. 4). These formulations are in principle extrudable on the Procusini printer and therefore used to study buildability. Buildability represents the shape stability of a material after deposition on a printing platform. It generally considers the resistance to deformation and potential of a material to build larger structures (Wilms et al., 2021). A buildable material has the strength to retain its stability after deposition (Godoi et al., 2016; Wilms et al., 2021; Zhu et al., 2019). Buildability can be studied by assessing the resistance to deformation of a 3D printed object. Liu et al. (2019) and Zhu et al. (2019) showed that the flow point (as determined by rheological analysis) could be related to the ability of a material to withstand the downward force exerted by the weight of the upper layers of a 3D printed object. Flow point was defined as the crossover point of elastic G′ and viscous G″ modulus (Liu et al., 2019; Zhu et al., 2019). It indicates the point at which a material starts behaving more viscous i.e., like a

liquid rather than a solid. In general, a lower flow point value corresponds to a lower shape stability after deposition on the printing platform and vice-versa.

Results of the effect of varying macronutrient composition on flow point are plotted in a ternary plot as shown in Fig. 6. There was a decrease in flow point, with an increase in fibre content up to 75%w/w db. This implies that samples with higher fibre content have a lower critical stress value. This is probably because the amount of weakly bound water is higher in samples with higher fibre content. Above 75% w/w db fibre content, the flow point appeared to slightly increase again, particularly when protein content was low (10%w/w db). This slight increase in flow point can be explained by the phase separation of water, which was also observed for extrusion force measurements (see section 3.2.1). Furthermore, the flow point increased with an increase in protein content which can be explained by the increase in viscosity of the continuous phase (as also mentioned in 3.2.1.). Finally, the flow point seemed to be unaffected by starch because it can be considered as an inert filler at the concentrations used in this study.

Zhu et al. (2019) quantified the stability of printed tomato puree and concentrate using multiple factors, including flow point and stress at collapse. Samples were printed until collapse and the stress experienced by the bottom layers was then calculated using the weight of the sample. Their results showed that flow point was directly correlated with stress at collapse. They reported relatively lower flow point values (<650Pa) compared to the pea-based formulations used in our study (>2000Pa). Since flow point values of our formulations were significantly higher, the samples did not collapse even when printed to a height of 50 mm due to which it was not possible to measure stress at collapse. Therefore, a higher flow point value is indicative of a higher print stability. Taking the aforementioned into consideration, one can conclude that the stability of a printed shape decreases with an increase in fibre content (20–80% w/w db), increases with an increase in protein content (10–50%w/w db), and remains unaffected with an increase in starch content (0–60%w/w db).

Overall, we observe a positive correlation between extrusion force and flow point ($R^2 = 0.889$). This result agrees with the findings reported by Zhu et al. (2019).

3.2.3. Printing precision

The quality of a 3D printed object is often qualitatively or semi-
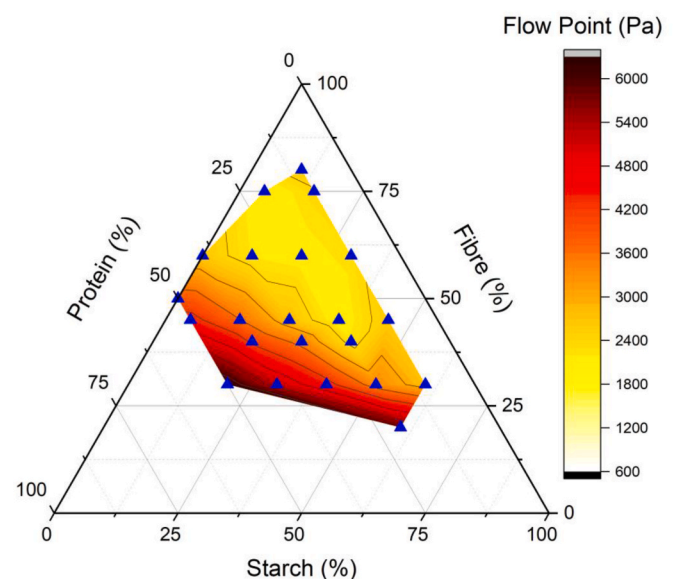

Fig. 6. Ternary plot showing the effect of varying macronutrients namely fibre, starch, and protein (dry basis) on sample shape stability after deposition on a printing platform.

quantitatively assessed. Lille, Nurmela, Nordlund, Metsä-Kortelainen, and Sozer (2018) used a visual scale of 1–5 to assess print quality in specific precision and shape stability. The lower end of the scale (1) represents poorly printed samples while the higher end (5) represents very well printed samples. Pant et al. (2021) adapted this scale to measure shape fidelity, structural integrity, and syneresis of printed fresh vegetables. Although these subjective approaches allow for a comparison of results from the same study, it is difficult to compare results from different studies. Therefore, we applied a new approach to quantify printing precision of printed food objects, by quantifying surface defect index (SDI). For this, white chocolate was chosen and printed as a reference sample (Fig. 7A). Pea-based samples were printed and compared with the reference white chocolate. Examples of three printed pea-based samples F40S40P20, F75S5P20, and F80S10P10 with good, medium, and poor printing precision are shown in Fig. 7B–D, respectively. With the same printing settings, a clear visual difference between the reference and test samples, as well as within test samples, was observed (Fig. 7A–D). To objectively quantify these visually observed differences, all the images were analyzed using canny edge detection (Fig. 7E–H). Printing precision was calculated by counting the number of white pixels observed in images processed with the Canny Edge Detector.

Visually, the reference, printed white chocolate had the highest number of continuous straight white lines (Fig. 7E) translating to having the lowest SDI score (normalized to zero). Sample F40S40P20 (Fig. 7F) had a comparable number of continuous straight-lined edges to the reference white chocolate while F75S5P20 (Fig. 7G) had a lower number. On the other hand, F80S10P10 (Fig. 7H) comparatively had a high number of discontinuous white lines. So, among these three printed pea-based samples, F40S40P20 had the highest number of white pixels, followed by F75S5P20 while F80S10P10 had the lowest. A larger number of white pixels translates to a relatively lower SDI i.e. higher printing precision and vice-versa. For example, white chocolate, F40S40P20, F75S5P20, and F80S10P10 shown in Fig. 7E–H have SDI values of 0, 0.051, 0.134, and 0.207, respectively. The SDI values are thus indicative for the level of visual surface defects. By following this methodology, 8% of the samples printed to a height of 50 mm were practically free of any surface defects (SDI <0.051), indicating a high printing precision compared with white chocolate. Although canny edge detection allows for quantification of printing precision (via the SDI value), the chosen threshold for acceptable printing precision is still subjective. For now, printing precision of object in Fig. 7C was chosen as

acceptable while that in Fig. 7D was considered to be coarse and therefore less acceptable. Having said this, of all the printed samples, 71% had an acceptable degree of surface effects (SDI <0.14), and 88% had a reasonable level of surface defects with the worst being less acceptable (SDI <0.20). Only a few samples (<12%) of the printable pea-based formulations can be considered very poorly printed (SDI>0.20). In the future, consumer studies can help define threshold SDI values for acceptability of such printed objects. This however is out-of-scope in this study.

Using the SDI values of all the samples that were printable to 50 mm height, a ternary plot was constructed (Fig. 8). An increase in fibre content did not seem to have a noticeable effect on SDI until a concentration of 75%w/w db. At around 80%w/w db, a slight increase was seen. This may be explained by the phase separation phenomenon as previously explained in 3.2.1. The phase separated water would leave
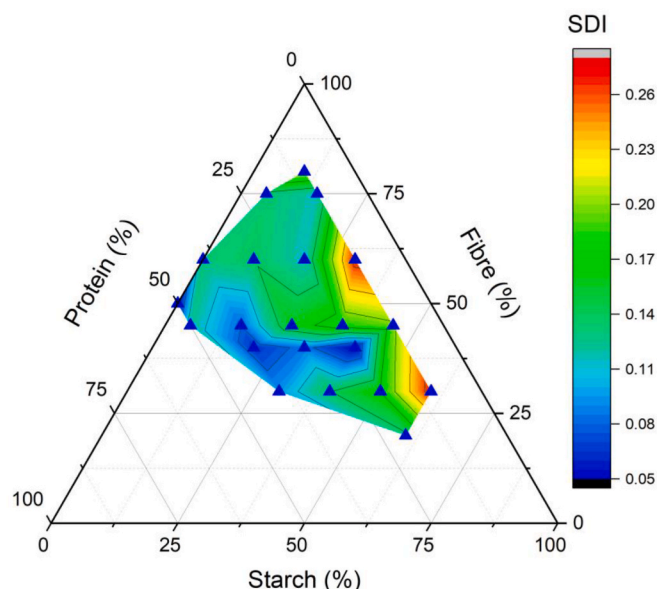

Fig. 8. Results quantifying printing precision in terms of surface defect index (SDI) after printing various pea-based compositions in the shape of a 40 × 40 × 50mm cuboid at a constant printing speed using a 1.2 mm nozzle.
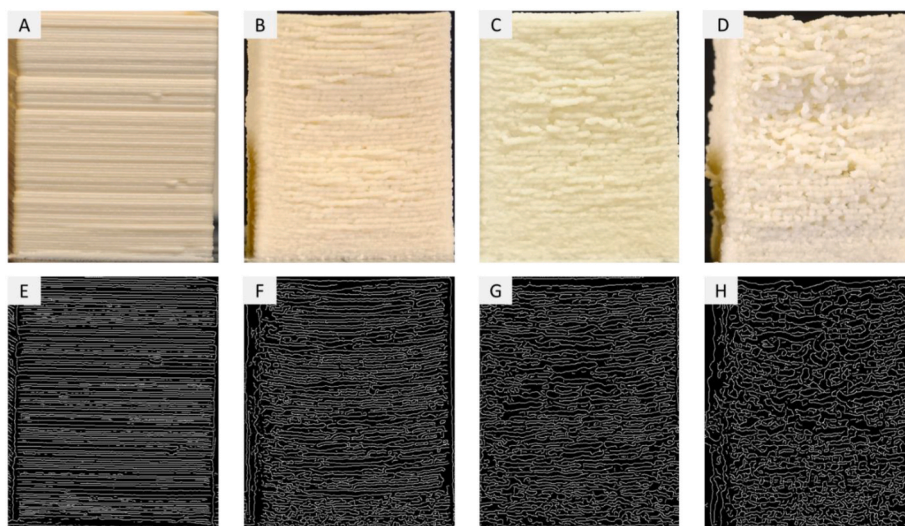

Fig. 7. A–D depict the frontal face of the 50 mm tall hollow cuboid printed with white chocolate, F40S40P20, F75S5P20, and F80S10P10, respectively. Visually, these samples have high, good, medium, and poor printing precision, respectively. E–H show the edges of the printed samples in A–D, respectively obtained after processing the image using a canny edge detection tool.

the nozzle with the dry ingredients in the initial layers. Therefore, the initial layers have a higher moisture content resulting in precisely printed layers. However, there is not sufficient water left in the remaining unprinted material in the cartridge to provide smooth continuous printing of the subsequent layers (Fig. 7D). These discontinuously printed layers result in a higher SDI. All these samples were printed and analyzed at constant printing settings to gain insights on the influence of macronutrient composition on printability. The printing precision of different objects may be affected by changing printing settings such as printing speed, printing pressure, the distance between the nozzle tip and the building platform and thus not varied (Naghieh, Sarker, Sharma, Barhoumi, & Chen, 2020; Schwab et al., 2020)

The SDI seemed to decrease with increasing protein content from 10 to 50%w/w db. Values of samples with 10%w/w db protein concentration appeared to be the lowest (Fig. 8). This observation depicts that irrespective of the amount of fibre and starch in the formulation, the amount of protein influences the printing precision the most. The CLSM image shown in Fig. 3A can be used to explain this phenomenon. At a low concentration of 10%w/w db, protein does not form the continuous phase of the matrix. At such low protein concentrations, depending on whether the formulation was dominated by fibre or starch, either phase separation or jamming effect was seen, respectively. At protein concentrations higher than 10%w/w db, starch did not seem to have a significant effect on SDI. These observations are in-line with the results of extrusion force and flow point.

Canny edge detection was applied to obtain a relatively simple quantitative measure of the surface quality of a printed object. This could be done on the condition that printing settings such as nozzle diameter, layer height, layer thickness were kept constant. Therefore, canny edge detection can be considered a viable method to quantitatively assess the printing precision of formulations studied here. From the SDI values (presented above), about 71% of the prepared printable pea-based inks could be printed with a good printing precision and even more (towards 88%) with reasonable printing precision. This result indicates that adding water based on the WHC of dry ingredients is an effective method to arrive at a printable landscape with minimal experimental effort.

4. Conclusion

Varying the composition of ingredients in water-based printing materials requires optimization of water content to obtain formulations with good printability. In this study, we developed a wide range of printable pea-based formulations varying in macronutrient composition by optimizing the water content. This optimization was based on the water holding capacity (WHC) of individual ingredients, thereby avoiding extensive trial-and-error. Printability of the developed formulations was evaluated in terms of extrudability (i.e. extrusion force), buildability (i.e. flow point), and printing precision (i.e. surface defect index). The extrudability of pea-based formulations was strongly influenced by their macronutrient composition, which was highly correlated to the buildability. Microscopic analysis using CLSM indicated that the formation of a continuous pea protein phase with dispersed insoluble pea fibre fibrils was a pre-requisite for good printability. When printing settings were kept the same, canny edge detection allowed for the quantification of printing precision. Printing precision of pea-based formulations varied per macronutrient composition. The results of this study highlight the importance of macronutrient composition in developing inks for personalized 3D food printing. The same workflow and quantitative insights obtained in this study can be used to develop other water-based formulations for extrusion-based 3D printing.

Author contributions

Aaditya Venkatachalam: Conceptualization, Methodology, Investigation, Validation, Formal analysis, Writing–original draft preparation, Writing–review & editing. Ajay Balasubramaniam: Conceptualization, Methodology, Formal analysis. Patrick Wilms: Conceptualization, Supervision, Validation, Writing–review & editing. Lu Zhang: Conceptualization, Supervision, Writing–review & editing, Funding acquisition. Maarten A.I. Schutyser: Conceptualization, Supervision, Writing–review & editing, Funding acquisition, Project administration.

Declaration of competing interest

The authors declare to have no conflicting interests.

Data availability

Data will be made available on request.

Acknowledgements

Appendix A. Supplementary data

Supplementary data to this article can be found online at https://doi.org/10.1016/j.foodhyd.2023.108760.

References

Barac, M., Cabrilo, S., Pesic, M., Stanojevic, S., Zilic, S., Macej, O., et al. (2010). Profile and functional properties of seed proteins from six pea (pisum sativum) genotypes. *International Journal of Molecular Sciences, 11*(12), 4973–4990.

Boulos, N. N., Greenfield, H., & Wills, R. B. H. (2000). Water holding capacity of selected soluble and insoluble dietary fibre. *International Journal of Food Properties, 3*(2), 217–231.

Celis-Morales, C., Livingstone, K. M., Marsaux, C. F., Macready, A. L., Fallaize, R., O`Donovan, C. B., et al. (2016). Effect of personalized nutrition on health-related behaviour change: Evidence from the Food4Me European randomized controlled trial. *International Journal of Epidemiology, 46*(2), 578–588.

Chuanxing, F., Qi, W., Hui, L., Quancheng, Z., & Wang, M. (2018). Effects of pea protein on the properties of potato starch-based 3D printing materials. *International Journal of Food Engineering, 14*(3).

Dekkers, B. L., de Kort, D. W., Grabowska, K. J., Tian, B., Van As, H., & van der Goot, A. J. (2016). A combined rheology and time domain NMR approach for determining water distributions in protein blends. *Food Hydrocolloids, 60*, 525–532.

Geerts, M. E. J., Dekkers, B. L., van der Padt, A., & van der Goot, A. J. (2018). Aqueous fractionation processes of soy protein for fibrous structure formation. *Innovative Food Science & Emerging Technologies, 45*, 313–319.

Godoi, F. C., Prakash, S., & Bhandari, B. R. (2016). 3d printing technologies applied for food design: Status and prospects. *Journal of Food Engineering, 179*, 44–54.

Morton, W. E., & Hearle, J. W. S. (1962). Physical properties of textile fibres. In *The textile institue and butterworth and Co* (1st ed. ed.). Publishers) Ltd.

He, C., Zhang, M., & Guo, C. (2020). *4D printing of mashed potato/purple sweet potato puree with spontaneous color change* (Vol. 59). Innovative Food Science & Emerging Technologies.

Kneifel, W., Paquin, P., Abert, T., & Richard, J. P. (1991). Water-holding capacity of proteins with special regard to milk proteins and methodological aspects—a review. *Journal of Dairy Science, 74*(7), 2027–2041.

Lille, M., Nurmela, A., Nordlund, E., Metsä-Kortelainen, S., & Sozer, N. (2018). Applicability of protein and fiber-rich food materials in extrusion-based 3D printing. *Journal of Food Engineering, 220*, 20–27.

Liu, Z., Bhandari, B., Prakash, S., Mantihal, S., & Zhang, M. (2019). Linking rheology and printability of a multicomponent gel system of carrageenan-xanthan-starch in extrusion based additive manufacturing. *Food Hydrocolloids, 87*, 413–424.

Liu, Y., Tang, T., Duan, S., Qin, Z., Zhao, H., Wang, M., et al. (2020). Applicability of rice doughs as promising food materials in extrusion-based 3D printing. *Food and Bioprocess Technology, 13*(3), 548–563.

Liu, Z., Zhang, M., & Ye, Y. (2020). Indirect prediction of 3D printability of mashed potatoes based on LF-NMR measurements. *Journal of Food Engineering, 287*.

Lorenz, T., Iskandar, M. M., Baeghbali, V., Ngadi, M. O., & Kubow, S. (2022). 3D food printing applications related to dysphagia: A narrative review. *Foods, 11*(12), 1789.

Ma, Y., Schutyser, M. A. I., Boom, R. M., & Zhang, L. (2021). Predicting the extrudability of complex food materials during 3D printing based on image analysis and gray-box

data-driven modelling. *Innovative Food Science & Emerging Technologies, 73*, Article 102764.

Moretti, M., Rossi, A., & Senin, N. (2021). In-process simulation of the extrusion to support optimisation and real-time monitoring in fused filament fabrication. *Additive Manufacturing, 38*, Article 101817.

Naghieh, S., Sarker, M., Sharma, N. K., Barhoumi, Z., & Chen, X. (2020). Printability of 3D printed hydrogel scaffolds: Influence of hydrogel composition and printing parameters. *Applied Sciences, 10*(1), 292.

O'Neill, R., McCarthy, H., Montufar, E. B., Ginebra, M.-P., Wilson, I., Lennon, A., et al. (2017). *Critical review: Injectability of calcium phosphate pastes and cements*.

Ordovas, J. M., Ferguson, L. R., Tai, E. S., & Mathers, J. C. (2018). Personalised nutrition and health. *BMJ, 361*, Article k2173. bmj.

Pant, A., Lee, A. Y., Karyappa, R., Lee, C. P., An, J., Hashimoto, M., et al. (2021). 3D food printing of fresh vegetables using food hydrocolloids for dysphagic patients. *Food Hydrocolloids, 114*.

Pereira, T., Barroso, S., & Gil, M. M. (2021). Food texture design by 3D printing: A review. *Foods, 10*(2).

Schwab, A., Levato, R., D'Este, M., Piluso, S., Eglin, D., & Malda, J. (2020). Printability and shape fidelity of bioinks in 3D bioprinting. *Chemical Reviews, 120*(19), 11028–11055.

Sura, L., Madhavan, A., Carnaby-Mann, G., & Crary, M. (2012). Dysphagia in the elderly: Management and nutritional considerations. *Clinical Interventions in Aging, 7*, 287–298.

Wang, J., Na, X., Navicha, W. B., Wen, C., Ma, W., Xu, X., et al. (2020). Concentration-dependent improvement of gelling ability of soy proteins by preheating or ultrasound treatment. *Lwt, 134*, Article 110170.

Wilms, P., Daffner, K., Kern, C., Gras, S. L., Schutyser, M. A. I., & Kohlus, R. (2021). Formulation engineering of food systems for 3D-printing applications – a review. *Food Research International, 148*, Article 110585.

Zayas, J. F. (1997). Water holding capacity of proteins. In J. F. Zayas (Ed.), *Functionality of proteins in food* (pp. 76–133). Berlin, Heidelberg: Springer Berlin Heidelberg.

Zhang, L., Lou, Y., & Schutyser, M. A. I. (2018). 3D printing of cereal-based food structures containing probiotics. *Food Structure, 18*, 14–22.

Zhu, S., Stieger, M. A., van der Goot, A. J., & Schutyser, M. A. I. (2019). *Extrusion-based 3D printing of food pastes: Correlating rheological properties with printing behaviour* (Vol. 58). Innovative Food Science & Emerging Technologies.